J|A|C|S COMMUNICATIONS

Published on Web 03/26/2009

Reversible Transformation between Rings and Coils in a Dynamic Hydrogen-Bonded Self-Assembly

Shiki Yagai,*[,†,‡] Shun Kubota,[†] Hikaru Saito,[†] Kanako Unoike,[†] Takashi Karatsu,[†] Akihide Kitamura,[†] Ayyappanpillai Ajayaghosh,[§] Masatoshi Kanesato,[||] and Yoshihiro Kikkawa*[,||]

Department of Applied Chemistry and Biotechnology, Graduate School of Engineering, Chiba University, 1-33 Yayoi-cho, Inage-ku, Chiba 263-8522, Japan, PRESTO, Japan Science Technology Agency (JST), 4-1-8 Honcho, Kawaguchi, Saitama 332-0012, Japan, Photosciences and Photonics Group, Chemical Science and Technology Division, National Institute for Interdisciplinary Science and Technology (NIIST), CSIR, Trivandrum-695019, India, and Photonics Research Institute, National Institute of Advanced Industrial Science and Technology (AIST), 1-1-1 Higashi, Tsukuba, Ibaraki 305-8562, Japan

Received January 24, 2009; E-mail: yagai@faculty.chiba-u.jp; y.kikkawa@aist.go.jp

Several proteins are known to exhibit unique dynamic self-organization processes involving ring-shaped and extended nanostructures triggered by chemical stimuli. An excellent example is tobacco mosaic virus coat protein, in which the ring (disk)-to-helical-coil transition can be regulated by pH or ionic strength even in the absence of RNA.[1] The β protein of the bacteriophage λ self-assembles into rings that are transformed into helically elongated filaments by the action of DNA.[2] Exploitation of synthetic molecular building blocks that show such smart self-organization processes leading to dynamically tunable nanostructures[3] is therefore an important step toward the mimicking of artificial biological systems.[4] Several self-assembling systems, such as amphiphilic triblock copolymers,[5] amphiphilic dumbbell-shaped small molecules,[6] proteins,[7] organometallic complexes,[8] and hydrogen-bonded supramolecular disks,[9] have been shown to spontaneously form ring-shaped nanostructures.[10] However, transformation of rings into coils as observed in biological assemblies has never been realized with artificial systems. Herein we demonstrate an unprecedented dynamic self-assembly of a synthetic rigid molecule into either nanorings or nanocoils driven by a concentration gradient in an aliphatic solvent.[11]

Compound **1**[12] consists of a barbituric acid (BAR) hydrogen-bonding headgroup, an oligo(*p*-phenylenevinylene) (OPV) π-conjugated segment,[13] and a wedge-shaped tridodecyloxybenzyl (TDB) tail (Figure 1).[14] **1** is considerably soluble ($c_{max} = 1 \times 10^{-3}$ M) in methylcyclohexane (MCH) upon gentle heating. The resulting orange solutions of **1** are stable for over 1 month. UV−vis spectra of the MCH solutions showed a strong hypochromic effect relative to those of THF solutions ($\varepsilon = 43\,100 \rightarrow 24\,300$ M^{-1} cm^{-1}; Figure S1 in the Supporting Information), indicating the self-assembly of **1**. Temperature-dependent UV−vis measurements in MCH ($c = 1 \times 10^{-5}$ M) gave a reversible spectral change between 60 and 110 °C, below which only a marginal spectral change was observed. This observation demonstrates the formation of fairly stable assemblies.

To our surprise, closed ring-shaped nanostructures (nanorings) were visualized by atomic force microscopy (AFM) analysis when **1** was drop-cast or spin-coated onto highly oriented pyrolytic graphite (HOPG) from an MCH solution at $c = 2 \times 10^{-5}$ M (Figure 2a). Spinning did not induce any morphological differences (Figures S2 and S3). The dimensions of nanorings were surprisingly uniform,

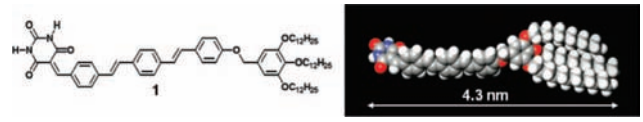

Figure 1. (left) Molecular structure and (right) CPK model of **1**.

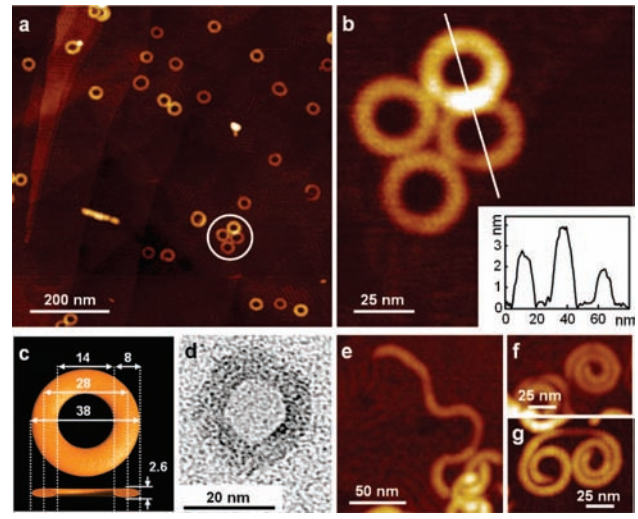

Figure 2. (a, b, e−g) AFM height images of a sample prepared by drop-casting of an MCH solution of **1** ($c = 2 \times 10^{-5}$ M) onto HOPG (z scale: 20 nm). Panel (b) is a magnified image of the circled region in (a), and its inset shows the cross section along the white line in (a). (c) Schematic illustration and typical dimensions (nm) of the nanoring as estimated by AFM. (d) TEM image of a single nanoring.

and the average values are shown in Figure 2c. The outer and inner diameters were typically 38 and 14 nm, respectively. The typical cross-sectional width and thickness were 8.0 and 2.6 nm, respectively,[15] demonstrating a flat, tapelike organization of **1**. Spontaneous formation of nanorings in solution without the aid of a dewetting process on the substrate[16] was evident from the observation of two partially overlapping nanorings, and the overlapping part gave a height of 4 nm (Figure 2b). This is further supported by the AFM observation using hydrophilic mica as a substrate, which showed almost the same ring-shaped nanostructures (Figure S4). Transmission electron microscopy (TEM) observations of the assemblies dip-coated on a carbon film also confirmed the formation of nanorings (Figure 2d and Figure S5).

Open-ended nanofibers with a variety of morphologies, such as curved fibers (Figure 2e), spirals (Figure 2f),[17] and double spirals

[†] Chiba University.
[‡] PRESTO, JST.
[§] NIIST.
[||] AIST.

10.1021/ja9005892 CCC: $40.75

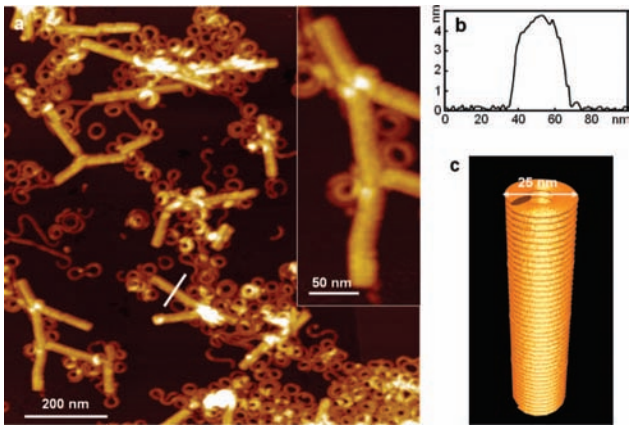

Figure 3. (a) AFM height images of a sample prepared by drop-casting of an MCH solution of **1** ($c = 1 \times 10^{-4}$ M) onto HOPG (z scale: 20 nm). (b) Cross section along the white line in (a). (c) Schematic illustration of a nanocoil constructed by coiling of open-ended fibers.

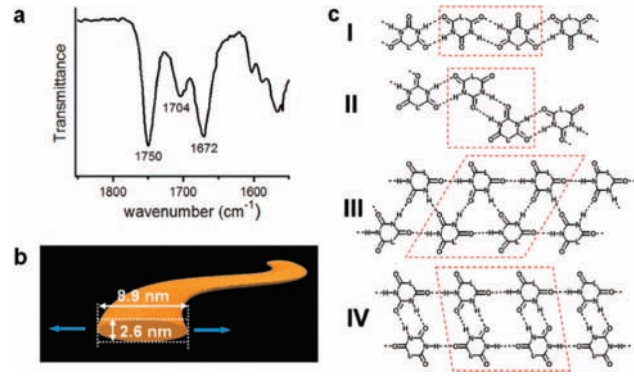

Figure 4. (a) FT-IR spectrum of a thin film of **1** prepared from its saturated MCH solution. (b) Schematic illustration of an open-ended fiber. Blue arrows indicate the direction of curvature. (c) Linear hydrogen-bonding motifs I−IV found from crystal structures of barbituric acid derivatives (see ref 21). The dimeric and tetrameric units surrounded by red dashed lines are possible oligomeric building blocks that may stack to form open-ended fibers.

with opposite rolling directions (Figure 2g), were found in the same sample as minor structures (10−20%). The formation of these curved nanostructures suggests that the existence of spontaneous curvature is encoded in the self-assembly of **1**. The open-ended nanostructures almost entirely disappeared when the concentration of **1** was decreased to less than 1×10^{-5} M by addition of solvent (Figure S6), revealing that the closed nanostructures are preferentially formed under diluted conditions. Although such a concentration-dependent ring−chain equilibrium has been reported in supramolecular polymers,[18] to the best of our knowledge, this has never been visualized for nanoscopic multiply hydrogen-bonded self-assemblies. The critical concentration is thus considered to be $\sim 2 \times 10^{-5}$ M.

When the concentration of **1** was increased to 4×10^{-5} M by evaporation of the solvent from the above solution, a considerable number (>70%) of open-ended nanostructures emerged (Figure S7). Remarkably, a further increase in the concentration to 1×10^{-4} M resulted in the evolution of rodlike nanostructures (nanorods) reminiscent of tobacco mosaic virus (Figure 3a). The contour lengths of the nanorods ranged from 100 to 300 nm, whereas the widths and the heights were uniform at ~25[15] and ~5 nm, respectively (Figure 3b). These short-axis dimensions did not vary from nanorod to nanorod, strongly suggesting that the rods are not formed by the bunching of open-ended fibers but instead are organized through their helical folding to form coils (Figure 3c).[19,20] The significant difference between the widths and the heights could be attributed to the hollow structure, which is susceptible to deformation by the evaporation process and the AFM tip force. The helical pitch may correspond to the thickness of the nanofibers, which was too short to be visualized by either AFM or TEM. These nanorods were transformed into rings when the concentration was decreased to 2×10^{-5} M by addition of solvent, demonstrating the reversible transformation between them. Coexistence of nanorods and other nanostructures persisted when the solution of **1** became saturated ($c = 1 \times 10^{-3}$ M; Figure S8).

Dynamic light scattering (DLS) measurements on MCH solutions of **1** at various concentrations corroborated the occurrence of the concentration-driven transformation of the nanostructures in solution. For the solution with $c = 2 \times 10^{-5}$ M, stable assemblies with hydrodynamic diameters (D_H) of ~60 nm were reproducibly detected in every measurement (Figure S9a), demonstrating the presence of discrete nanostructures. In a larger-sized region, assemblies having irregular D_H values were randomly observed, which could be attributed to the existence of open-ended assemblies. At $c = 4 \times 10^{-4}$ M, nanorings were still observed, but the D_H values of the other assemblies lacked reproducibility between the measurements (Figure S9b), reflecting the formation of flexible open-ended assemblies with nonequilibrated morphologies. Notably, a further increase in the concentration to 1×10^{-4} M led to the integration of the D_H of the randomly observed assemblies into the 100−300 nm range (Figure S9c). This observation clearly shows the evolution of nanorods with a relatively narrow size distribution in their counter lengths (see Figure 3a).

Diverse hydrogen-bonding motifs have been found for numerous single crystals of 5,5-disubstituted BAR derivatives.[21] FT-IR studies have shown that the C═O stretching vibrations of BAR moieties in their single crystals are sensitive to the hydrogen-bonding motifs.[22] A thin film of **1** prepared from its saturated MCH solution containing all the aforementioned nanostructures exhibited three sharp C═O stretching vibrations at 1750, 1704, and 1672 cm^{-1} (Figure 4a) ascribable to the three C═O groups. Thus, only one type of hydrogen-bonding motif is responsible for producing all of the nanostructures of **1**.

Open-ended fibers (Figure 2e) are obviously the intermediate species between nanorings and nanorods. They have a tapelike morphology with a thickness of 2.6 nm and a width of 8.9 nm (Figure 4b). Of the diverse hydrogen-bonding motifs found for BAR derivatives, the one-dimensional ones listed in Figure 4c are candidates that could be responsible for the open-ended fibers.[21] However, it seems unlikely that self-assemblies of **1** comprising such rigid hydrogen-bonding motifs would curve sharply in the lateral direction (blue arrows in Figure 4b). The rings, which measure 29 nm in body-to-body width, are formed by ring closure of fibers measuring 91 nm in length, and this process apparently involves significant strain energy. Furthermore, molecular modeling showed that neighboring OPV segments in the self-assemblies of **1** based on these hydrogen-bonding motifs are separated by at least 6 Å, which does not permit the strong π-electronic interactions observed by UV−vis spectroscopy. We thus believe that a different type of supramolecular organization occurs with **1**.

When the thin film of **1** was heated above 230 °C, a liquid-crystalline mesophase was observed up to 250 °C by differential scanning calorimetry and polarized optical microscopy. X-ray diffraction of the mesophase confirmed the formation of a body-centered rectangular columnar (Col_r) structure with lattice constants $a = 8.3$ nm and $b = 7.5$ nm (Figure S10). The formation of a Col_r structure strongly suggests discotic association of **1** followed by stacking of the resulting disks with translational and most likely

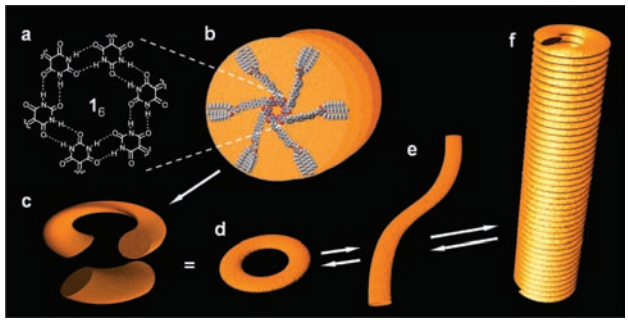

Figure 5. Schematic illustration of a proposed mechanism for organization of **1** into nanorings, open-ended nanofibers, and nanocoils through the cyclic hexamer $\mathbf{1}_6$.

rotational displacements, affording columns with an ellipsoidal cross-section that favors rectangular packing in the bulk state.[23] For such a disk, dimeric or tetrameric units in the linear hydrogen-bonding motifs shown in Figure 4c can be potential candidates.[24] However, these oligomeric units possess at least two free NHCO hydrogen-bonding sites, the presence of which is enthalpically unfavorable in aliphatic solvents. We rather propose that a hexameric disk of **1** ($\mathbf{1}_6$) shown in Figure 5a is the primary supramolecular species in the present system.

The complex self-organization process of **1** is summarized in Figure 5. In aliphatic solvents, columnar stacks of $\mathbf{1}_6$ are isolated by solvation and behave as tapelike nanofibers (Figure 5e). At concentrations below 2×10^{-5} M, the lengths of columns are moderate (~90 nm as judged from the circumferences of the nanorings), allowing intrachain end-to-end interactions to form rings (Figure 5d). Such a ring closure of short columns consisting of π-conjugated supramolecular disks (rosettes) is similar to our earlier observation that the oligo(*p*-phenyleneethynylene) rosette provides nanorings with widths of 40 nm as a result of "biased stacking" between the rosettes.[9] In the present case, it is most likely that translational and rotational offsets upon stacking of $\mathbf{1}_6$ units are responsible for the spontaneous curvature of columns (Figure 5b,c). A surprising uniformity in the size of the present nanorings indicates that such offsets between $\mathbf{1}_6$ disks evolve with a specific distance and angle. At concentrations above 1×10^{-4} M, the columns further extend over 200 nm, which eventually leads to their folding into nanorods to minimize the surface free energy (Figure 5f).

The perfect morphological features of the present nanorings and nanorods make them particularly attractive as nanomaterials with unique electronic, magnetic, and optical properties. Further investigation of the packing structure, selective formation of a single nanostructure through changes in the external environment (e.g., solvent), exploration of their conductive properties, and the diversification of nanostructures by addition of complementary melamine components[25] are currently underway and will be reported in due course.

Acknowledgment. S.Y. thanks the Futaba Electronics Memorial Foundation and the Nanohana Competition of Chiba University for valuable discussions and financial support. S.Y., A.A., and A.K. thank the Japan Society for the Promotion of Science, Japan, and the Department of Science and Technology, New Delhi, for financial support. We also thank the referees of this paper for their valuable suggestions.

Supporting Information Available: Synthesis of **1** and UV−vis, TEM, AFM, DLS, and XRD data for the assemblies. This material is available free of charge via the Internet at http://pubs.acs.org.

References

(1) Klug, A. *Angew. Chem.* **1983**, *95*, 579–596.
(2) Passy, S. I.; Yu, X.; Li, Z.; Radding, C. M.; Egelman, E. H. *Proc. Natl. Acad. Sci. U.S.A.* **1999**, *96*, 4279–4284.
(3) (a) Ajayaghosh, A.; Praveen, V. K. *Acc. Chem. Res.* **2007**, *40*, 644–656. (b) Ajayaghosh, A.; Chithra, P.; Varghese, R. *Angew. Chem., Int. Ed.* **2007**, *46*, 230–233. (c) Ryu, J.-H.; Kim, H.-J.; Huang, Z.; Lee, E.; Lee, M. *Angew. Chem., Int. Ed.* **2006**, *45*, 5304–5307. (d) Nakanishi, T.; Schmitt, W.; Michinobu, T.; Kurth, D. G.; Ariga, K. *Chem. Commun.* **2005**, 5982–5984.
(4) Whitesides, G. M.; Grzybowski, B. *Science* **2002**, *295*, 2418–2421.
(5) (a) Pochan, D. J.; Chen, Z.; Cui, H.; Hales, K.; Qi, K.; Wooley, K. L. *Science* **2004**, *306*, 94–97. (b) Zhu, J.; Liao, Y.; Jiang, W. *Langmuir* **2004**, *20*, 3809–3812.
(6) Kim, J.-K.; Lee, E.; Huang, Z.; Lee, M. *J. Am. Chem. Soc.* **2006**, *128*, 14022–14023.
(7) Carlson, J. C. T.; Jena, S. S.; Flenniken, M.; Chou, T.-f.; Siegel, R. A.; Wagner, C. R. *J. Am. Chem. Soc.* **2006**, *128*, 7630–7638.
(8) Lu, W.; Chui, S. S.-Y.; Ng, K.-M.; Che, C.-M. *Angew. Chem., Int. Ed.* **2008**, *47*, 4568–4572.
(9) Yagai, S.; Mahesh, S.; Kikkawa, Y.; Unoike, K.; Karatsu, T.; Kitamura, A.; Ajayaghosh, A. *Angew. Chem., Int. Ed.* **2008**, *47*, 4691–4694.
(10) For a review of other ring-shaped nanostructures, see: Vossmeyer, T.; Chung, S.-W.; Gelbart, W. M.; Heath, J. R. *Adv. Mater.* **1998**, *10*, 351–353.
(11) For an example of concentration-driven transformation of nanostructures, see: Ajayaghosh, A.; Varghese, R.; Praveen, V. K.; Mahesh, S. *Angew. Chem., Int. Ed.* **2006**, *45*, 3261–3264.
(12) For synthesis and characterization details, see the Supporting Information.
(13) Selected examples of self-assembling OPVs: (a) Ajayaghosh, A.; George, S. J. *J. Am. Chem. Soc.* **2001**, *123*, 5148–5149. (b) Jonkheijm, P.; Miura, A.; Zdanowska, M.; Hoeben, F. J. M.; De Feyter, S.; Schenning, A. P. H. J.; De Schryver, F. C.; Meijer, E. W. *Angew. Chem., Int. Ed.* **2004**, *43*, 74–78. (c) Messmore, B. W.; Hulvat, J. F.; Sone, E. D.; Stupp, S. I. *J. Am. Chem. Soc.* **2004**, *126*, 14452–14458. (d) Tomović, Z.; van Dongen, J.; George, S. J.; Xu, H.; Pisula, W.; Leclère, P.; Smulders, M. M.; De Feyter, S.; Meijer, E. W.; Schenning, A. P. H. J. *J. Am. Chem. Soc.* **2007**, *129*, 16190–16196. (e) Yagai, S.; Kubota, S.; Iwashima, T.; Kishikawa, K.; Nakanishi, T.; Karatsu, T.; Kitamura, A. *Chem.—Eur. J.* **2008**, *14*, 5246–5257.
(14) Beginn, U.; Keinath, S.; Möller, M. *Liq. Cryst.* **1997**, *23*, 35–41.
(15) These were the values after reducing the tip broadening factor (see Supporting Information for details).
(16) Schenning, A. P. H. J.; Benneker, F. B. G.; Geurts, H. P. M.; Liu, X. Y.; Nolte, R. J. M. *J. Am. Chem. Soc.* **1996**, *118*, 8549–8552.
(17) A barbituric acid derivative has been reported to form spiral nanostructures in an LB film: Huang, X.; Li, C.; Jiang, S.; Wang, X.; Zhang, B.; Liu, M. *J. Am. Chem. Soc.* **2004**, *126*, 1322–1323.
(18) ten Cate, A. T.; Sijbesma, R. P. *Macromol. Rapid Commun.* **2002**, *23*, 1094–1112.
(19) For reviews, see: (a) Hill, D. J.; Mio, M. J.; Prince, R. B.; Hughes, T. S.; Moore, J. S. *Chem. Rev.* **2001**, *101*, 3893–4011. (b) Zhao, D.; Moore, J. S. *Org. Biomol. Chem.* **2003**, *1*, 3471–3491.
(20) Examples of self-assembled nanocoils formed by π-conjugated molecules: (a) Lovinger, A. J.; Nuckolls, C.; Katz, T. J. *J. Am. Chem. Soc.* **1998**, *120*, 264–268. (b) Engelkamp, H.; Middelbeek, S.; Nolte, R. J. M. *Science* **1999**, *284*, 785–788. (c) Hill, J. P.; Jin, W.; Kosaka, A.; Fukushima, T.; Ichihara, H.; Shimomura, T.; Ito, K.; Hashizume, T.; Ishii, N.; Aida, T. *Science* **2004**, *304*, 1481–1483. (d) Ajayaghosh, A.; Vijayakumar, C.; Varghese, R.; George, S. J. *Angew. Chem., Int. Ed.* **2006**, *45*, 456–460. (e) Yang, W.-Y.; Lee, E.; Lee, M. *J. Am. Chem. Soc.* **2006**, *128*, 3484–3485.
(21) MacDonald, J. C.; Whitesides, G. M. *Chem. Rev.* **1994**, *94*, 2383–2420.
(22) (a) Cleverley, B.; Williams, P. P. *Tetrahedron* **1959**, *7*, 277–288. (b) Craven, B. M.; Vizzini, E. A.; Rodrigues, M. M. *Acta Crystallogr.* **1969**, *B25*, 1978–1993.
(23) (a) Jin, S.; Ma, Y.; Zimmerman, S. C.; Cheng, S. Z. D. *Chem. Mater.* **2004**, *16*, 2975–2977. (b) Yagai, S.; Nakajima, T.; Kishikawa, K.; Kohmoto, S.; Karatsu, T.; Kitamura, A. *J. Am. Chem. Soc.* **2005**, *127*, 11134–11139.
(24) Zubarev, E. R.; Sone, E. D.; Stupp, S. I. *Chem.—Eur. J.* **2006**, *12*, 7313–7327.
(25) Yagai, S.; Kinoshita, T.; Higashi, M.; Kishikawa, K.; Nakanishi, T.; Karatsu, T.; Kitamura, A. *J. Am. Chem. Soc.* **2007**, *129*, 13277–13287.

JA9005892